PERGAMON

International Journal of Heat and Mass Transfer 42 (1999) 2031–2040

International Journal of HEAT and MASS TRANSFER

Heat transfer efficiency of metal honeycombs

T.J. Lu*

Department of Engineering, University of Cambridge, Cambridge CB2 1PZ, U.K.

Received 19 June 1998; in final form 21 August 1998

Abstract

The efficiency of micro-cell aluminium honeycombs in augmenting heat transfer in compact heat exchangers is evaluated using analytical models. For convective cooling, the overall heat transfer rate is found to be elevated by about two order of magnitudes when an open channel is designed with an aluminium honeycomb core. The performance is comparable to that achieved by using open-celled aluminium foams, but attributed to different mechanisms. At low Reynolds numbers (<2000), the flow is essentially laminar in honeycombs, in contrast to the largely turbulent flow in metal foams; this deficiency in fluid dynamics is compensated for by the superior surface area density offered by honeycombs over foams. Another advantage of designing heat sinks with honeycombs is the relatively small pressure drop experienced and minimal noise generated by the laminar flow. The overall heat transfer rate of the heat sink is maximised when the cell morphology of the honeycomb is optimised. However, the optimal cell morphology is not constant but dependent upon the geometry and heat transfer condition of the heat sink as well as the type of convective cooling medium used. For air cooling, the optimal relative density of the honeycomb is about 0.1. Other related effects, such as cell orientation and double cell wall thickness, are discussed.

Nomenclature

a cell size
Bi Biot number
c_p specific heat
D_h hydraulic diameter
f friction factor
h local heat transfer coefficient
$\bar{h}$ overall heat transfer coefficient
H, L, W thickness, length and width of sandwich heat exchanger
I dimensionless scaling index
l cell wall length
(L^*, x^*) characteristic length scales
m $\equiv\sqrt{2Bi/t}$
$\dot{m}$ mass flow rate
Nu Nusselt number, hD_h/λ_f
$(p, \Delta p)$ pressure and pressure drop
Pr Prandtl number, $c_p\mu_f/\lambda_f$
q heat flux
Q total heat transfer rate
Re Reynolds number, $v_f D_h/v_f$
t cell wall thickness
T, $\bar{T}$ temperature and its average
v velocity
(x, y, z) global Cartesian coordinates.

Greek symbols

ΔT_m logarithmic mean temperature difference
λ thermal conductivity
(ξ, η) local coordinates along cell walls
μ shear viscosity
v kinematic viscosity
ρ density.

Subscripts

e exit of heat sink
f fluid
s solid
w plate wall
0 inlet of heat sink.

1. Introduction

Traditionally, honeycombs made of metals have been mainly used as the core of sandwich panels for highly

* Tel.: 0044 1223 766316; fax: 0044 1223 332662; e-mail: tjl21@eng.cam.ac.uk

0017–9310/99/$ - see front matter
PII: S0017–9310(98)00306–8

engineered structural applications where high strength at minimum weight are required (e.g., aircraft and snow/water skis). Recent advances in low-cost processing have enabled the fabrication of corrosion resistant aluminium honeycombs having cell sizes on the order of 1 mm [1]. The surface area to volume ratio (i.e., the surface area density) of a typical micro-cell honeycomb is about 3000 $m^2\ m^{-3}$, making them ideal candidates for compact heat exchanger applications where high surface area density is required (e.g., electronic packages and airborne devices).

For nearly two decades, numerous efforts have been spent on developing innovative heat dissipation media for high power electronics. These include micro-channels and pin-fin arrays [2, 5, 11, 12]. More recently, it has been demonstrated both theoretically and experimentally that, when cooled by forced convection, three-dimensional open-celled metal foams attached to a heated substrate comprise a compact and highly efficient heat dissipation medium for high power electronics [2–5]. This, together with the cooling concepts at the device level (micro-channel heat pipes [6]) and at the assembly level (highly conducting heat spreaders [7]), complete the three critical elements in the thermal management of increasingly powerful electronic packages which demand power densities in excess of $10^7\ W\ m^{-2}$. Are aluminium honeycombs good compact heat exchangers? At the same relative density level, how are they competing with the three-dimensional open-cell metal foams such as ERG (trade name Duocel)? Does there exist an optimal cell morphology which would maximise the heat transfer efficiency of a metallic honeycomb? Answers to these questions will be provided in this paper.

2. The model

The prototype problem considered is shown in Fig. 1(a), where the cooling of a compact multi-chip module is enhanced by forced convective flow across a metal honeycomb medium of thickness H sandwiched between two flat rectangular plates of length L and width W. The honeycomb consists of regular hexagonal cells of cell size $a = \sqrt{3}l$, cell wall length l and thickness t (Fig. 1(b)). Let λ_s and ρ_s be the thermal conductivity and density of the solid of which the cell wall is made. The plates holding the chips are assumed to be thin and have large thermal conductivity so that the through-thickness heat conduction may be neglected. The module is thermally insulated at the top ($z = 0$) and bottom ($z = H$) by protective covers (not shown in Fig. 1(a)) and, without loss of generality, it is assumed that the sandwich structure is capped and thermally insulated at both ends $y = W/2$ and $y = -W/2$. Two types of heat transfer boundary conditions are prescribed: Type I applies when both plates are isothermal with uniform temperature T_w whereas Type II holds if the plates release uniform heat flux (isoflux) q_0 to the fluid-saturated porous medium. It is expected that these two boundary conditions lead to lower and upper bound solutions to the problem. Cooling fluid, velocity v_0, temperature T_0 ($< T_w$) and pressure p_0, is forced into the honeycomb at the inlet ($x = 0$) and exits at the outlet ($x = L$) with temperature T_e and pressure p_e. The width of the channel, W, is assumed to be much larger than the cell size a so that the thermal and hydraulic fields are independent of the coordinate y.

It proves convenient to divide the prototypical heat sink into slices of equal width, as illustrated in Fig. 1(c) for a honeycomb having uniform cell wall thickness and with two of the cell walls oriented parallel to the plate surfaces—cells with double wall thickness and oriented different from that shown in Fig. 1 will be considered later. Each slice consists of a corrugated wall with fins each of length $l/2$ attached at periodic position, distance $a/2$ apart, along the wall. Symmetry considerations dictate that the fins are all thermally insulated at the tips. The total number of such slices in the heat sink is $2W/3l$. Let h be the average heat transfer coefficient associated with the corrugated wall and let $T(x, z)$ be the solid temperature averaged over the cross-sectional area of the wall at location x. (As $t \ll l$ for most metallic honeycombs, the variation of T across the cell wall thickness may be neglected.) Let λ_f, ρ_f, ν_f, μ_f and c_p denote the thermal conductivity, density, kinematic viscosity, shear viscosity and specific heat at constant pressure of the fluid, respectively. The usual assumptions of steady state, and constant thermal/physical properties of both fluid and solid are made. In the subsequent sections of the paper, we shall consider the following problems, all posed for the thermal model of Fig. 1:

- overall heat transfer efficiency of the system under Type I condition;
- overall heat transfer efficiency of the system under Type II condition;
- effects of cell orientation and double cell wall thickness;
- optimal cell size and relative density for best heat transfer performance.

3. Isothermal surfaces

The heat transfer analysis is based on the corrugated wall model shown in Fig. 1(c) and is accomplished in two steps. First, we neglect the effects of fin attachments to obtain the heat lost to the cooling fluid from a single corrugated wall; the result is then modified to include the additional heat loss from the fins. The thermal fields of the entire heat sink are obtained subsequently using an energy balance method similar to that described in [2]. To complete the model, other related issues such as local heat transfer coefficient, characteristic length scale,

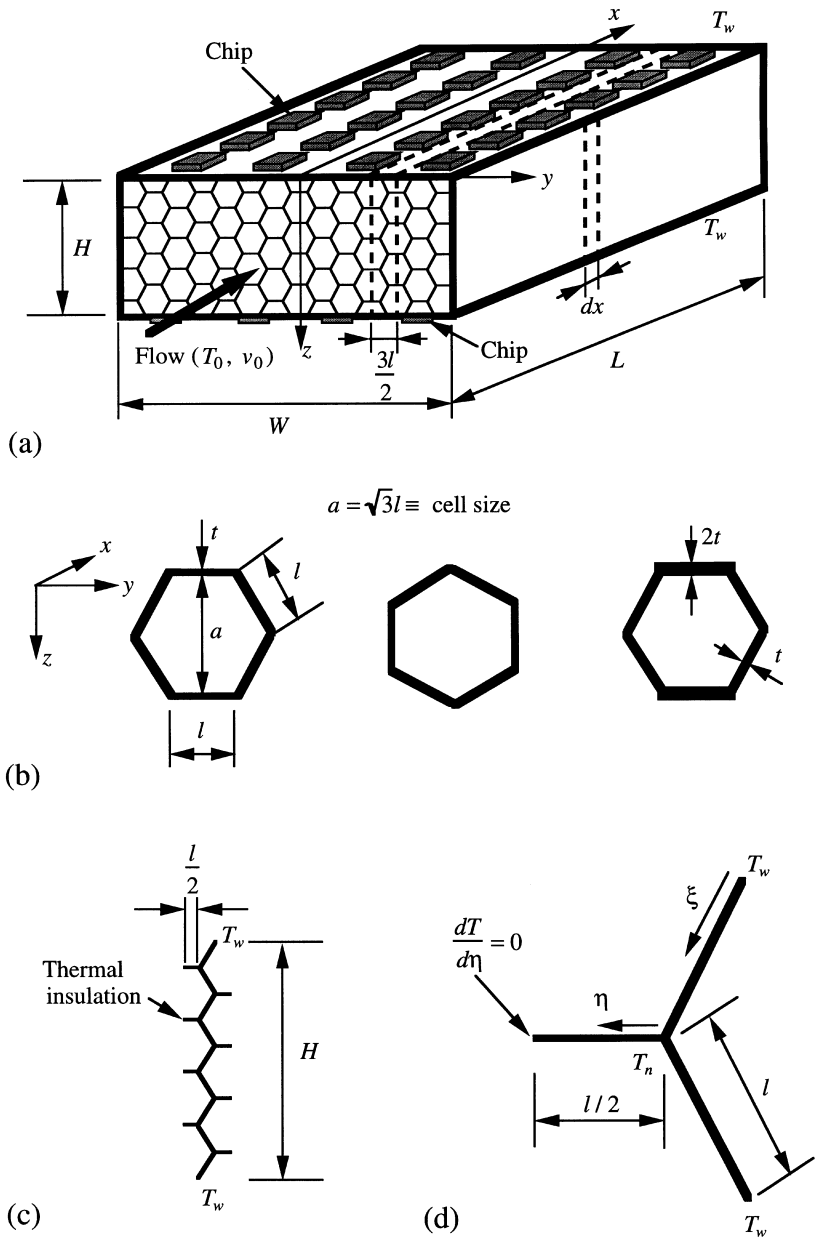

Fig. 1. A prototypical design of compact multi-chip module cooled by forced convection through metal honeycomb: (a) notations; (b) hexagonal cells with two horizontal walls, two vertical walls and two double thickness horizontal walls, respectively; (c) corrugated wall with fin attachments; and (d) definition of local coordinates. The heat transfer boundary condition shown is isothermal temperature on the substrate surfaces.

pressure drop and overall heat transfer coefficient are discussed.

3.1. A single corrugated wall without fins

With reference to Fig. 1(c), it is straightforward to show that, in the absence of fin attachments, the variation of temperature T along the length of a single corrugated wall is governed by

$$\frac{d^2T}{d\xi^2} - \frac{2h}{\lambda_s t}(T - T_f) = 0 \tag{3.1}$$

where $T_f(x)$ is the mean fluid temperature at location x (to be determined later in Section 3.3) and $\xi = 2z/\sqrt{3}$ is

the local coordinate along the wall with the origin $\xi = 0$ coinciding with $z = 0$. The effects of radiation at the wall surface can be shown to be small, hence neglected in the derivation of equation (3.1). Subjected to the boundary condition that $T = T_w$ at $\xi = 0$ and at $\xi = 2H/\sqrt{3}$, equation (3.1) can be solved to arrive at

$$T(x,\xi) = T_f(x) + (T_w - T_f(x)) \times \frac{\cosh\{\sqrt{2\,Bi}(H/\sqrt{3} - \xi)/t\}}{\cosh(\sqrt{2Bi/3}H/t)} \quad (3.2)$$

where $Bi = ht/\lambda_s$ is the Biot number. It is expected that $Bi \ll 1$ for typical aluminium honeycombs. The average wall temperature is

$$\bar{T}(x) = T_f(x) + (T_w - T_f(x)) \frac{\tanh(\sqrt{2\,Bi/3}H/t)}{\sqrt{2\,Bi/3}H/t}. \quad (3.3)$$

Thus, $\bar{T}(x) \to T_f(x)$ if $Bi \to 0$ and $\bar{T}(x) \to T_w$ if $Bi \to \infty$. The total heat lost to the cooling medium per unit length of the corrugated wall is

$$q_1 = -2\lambda_s t \left.\frac{dT}{d\xi}\right|_{\xi=0} = 2\sqrt{2\,Bi}\,\lambda_s (T_w - T_f)\tanh(\sqrt{2\,Bi/3}H/t). \quad (3.4)$$

Note that $q_1 \neq -2\lambda_s t(dT/dz)|_{z=0}$.

3.2. Effects of fins

The contribution to heat loss from fin attachments is analysed below. For simplicity, consider a honeycomb heat sink having the same geometry as shown in Fig. 1(a) but with only one cell across the thickness (in the z-direction). A slice of the heat sink with width $3l/2$ is shown in Fig. 1(d) for which exact solutions for the variation of temperature $T(x,\xi)$ along the corrugated wall and $T(x,\eta)$ along the fin can be obtained. The local coordinates ξ and η are defined in Fig. 1(d). For $T(x,\xi)$, the governing equation is still given by equation (3.1), but the heat transfer boundary conditions are different: $T = T_w$ at $\xi = 0$ and $T = T_n$ at $\xi = l$, T_n being the unknown temperature at the junction between the wall and fin. With ξ replaced by η, equation (3.1) also governs the variation of fin temperature $T(x,\eta)$; the corresponding boundary conditions are $T = T_n$ at $\eta = 0$ and $dT/d\eta = 0$ at $\eta = l/2$. In addition, energy balance dictates that $dT/d\eta = 2dT/d\xi$ at $\eta = 0$ (or, equivalently, at $\xi = l$). The solutions are

$$T(x,\xi) = T_f(x) + (T_w - T_f(x))\left\{\cosh m\xi + \sinh m\xi \frac{[\cosh ml + \sinh^2(ml/2)]^{-1} - \cosh ml}{\sinh ml}\right\} \quad (3.5a)$$

and

$$T(x,\eta) = T_f(x) + (T_w - T_f(x)) \times \frac{\cosh[m(l/2-\eta)]}{\cosh(ml/2)[\cosh ml + \sinh^2(ml/2)]} \quad (3.5b)$$

where $m = \sqrt{2\,Bi}/t$. The total heat loss (per unit length) from both the corrugated wall and the fin is

$$q' = 2\lambda_s mt(T_w - T_f) \times \frac{\cosh(ml) - [\cosh(ml) + \sinh^2(ml/2)]^{-1}}{\sinh(ml)}. \quad (3.6)$$

Similar exact solutions can be obtained for a corrugated wall with many fins (Fig. 1(c)), but the resulting expression is tedious and much less revealing. An approximate solution which would correlate closely with equation (3.6) while maintaining the simplicity of equation (3.4) is attempted, as follows. In the absence of the fin, the solution to the problem shown in Fig. 1(d) follows directly from equation (3.4) as

$$q_1 = 2\lambda_s mt(T_w - T_f)\tanh(ml). \quad (3.7a)$$

The length of the fin is 1/4 of that of the corrugated wall, hence it is expected that the additional heat loss from the fin is about $q_1/4$, with the assumption that the average fin temperature in a micro-cell of size ~ 1 mm may be approximated by the average temperature attained by the corrugated wall. The (approximate) solution for the total heat loss per unit thickness of the slice may therefore be written as

$$q = (1 + 1/4)2\lambda_s mt(T_w - T_f)\tanh(ml). \quad (3.7b)$$

When $0.1 < ml < 1$, an error less then 10% is incurred by replacing q' of equation (3.6) with q of equation (3.7b). For micro-cell aluminium honeycombs subjected to forced air or water cooling, $ml = 0.1 \sim 0.5$, hence the approximation $q \approx q'$ is appropriate. For a corrugated wall with many fin attachments (Fig. 1(c)), the total fin length is half that of the wall without fins; the approximate solution for q follows therefore from equation (3.4) as

$$q = 3\sqrt{2\,Bi}\,\lambda_s(T_w - T_f)\tanh(\sqrt{2\,Bi/3}H/t. \quad (3.8)$$

3.3. Mean fluid temperature T_f and characteristic length scale L*

The fluid temperature inside the heat sink is, in general, dependent upon the spatial coordinates x, y and z. It is coolest at the inlet and hottest at the outlet; also, a boundary layer develops near the plate surface with the fluid layer situated closer to the plate warmer than a layer farther away from the plate. The present analysis does not attempt to find the detailed temperature field of the fluid everywhere in the heat sink, given its complicated cellular microstructure. A simple model is used to solve for the steady-state distribution of the average fluid temperature inside the heat sink, with the assumption that heat transfer between the fluid and solid cell wall is gov-

erned by a constant heat transfer coefficient h obtainable from laminar flow in a hexagonal duct (Section 3.4). As is customary in the heat transfer analysis of ducts [7], a mean temperature $T_f(x)$ of the fluid is defined over the cross-section of the honeycomb at location x = fixed, such that for the control volume of length dx (Fig. 1(a)):

$$\dot{m}c_p[T_f(x+dx)-T_f(x)]=(dx)[N_s q(x)+q_w(x)] \tag{3.9}$$

where $N_s = 2W/3l$ is the total number of slices and

$$q_w(x) = 2h(W-N_s\sqrt{3}t/2)[T_w-T_f(x)] \tag{3.10}$$

is the heat flux into the fluid from both plates per unit length excluding attributes of the honeycomb. Thus, T_f is the average temperature that satisfies the First Law of Thermodynamics.

The combining of equations (3.8)–(3.10) gives rise to an ordinary differential equation for the mean fluid temperature $T_f(x)$. The solution is

$$T_f(x) = T_w-(T_w-T_0)\exp(-x/L^*) \tag{3.11}$$

where L^* is the characteristic length scale of the problem given by

$$L^* = \frac{\rho_f c_p v_0 H}{2h}\left\{1-\frac{t}{a}+\frac{t}{a}\sqrt{\frac{6}{Bi}}\tanh(\sqrt{2\,Bi/3}H/t)\right\}^{-1}. \tag{3.12}$$

From equation (3.11), the average fluid temperature inside the heat sink of height H, width W and length L is obtained as

$$\bar{T}_f = T_0+(T_w-T_0)\left\{1-\frac{L^*}{L}[1-\exp(-L/L^*)]\right\}. \tag{3.13}$$

Notice that in the limit $L/L^*\to\infty$, $\bar{T}_f\to T_w$.

3.4. Local heat transfer coefficient h and pressure drop Δp

Heat transfer in a uniform duct of arbitrary cross-sectional area is characterised by the Nusselt number, $Nu = hD_h/\lambda_f$ which, according to simple dimensional arguments, is a function of the Reynolds number, $Re = v_f D_h/\nu_f$, and the Prandtl number, $Pr = c_p\mu_f/\lambda_f$. Here, v_f is the average flow velocity inside the duct and D_h is the hydraulic diameter, with $D_h = a$ for a regular hexagonal cross-section. When $Re < 2000$, the flow is laminar. For micro-cell honeycombs having cell sizes ~ 1 mm, this is a valid assumption under most circumstances.

The Nusselt number for laminar flow in a regular hexagonal duct with constant wall temperatures is proportional to $((x/D_h)/Re\,Pr)^{-0.5}$ in the entrance region of the duct ($Nu \approx 8$ when $(x/D_h)/Re\,Pr \ll 1$), and attains its fully developed value 3.353 when $Re\,Pr$ is approximately 0.1 [7–9]. Therefore, for air and water, the entrance region has a length about 10–50 times the cell size a. The present analysis neglects the effects of developing flows at the entrance to the heat sink, and assumes an average heat transfer coefficient given by

$$h = 3.353\frac{\lambda_f}{a}. \tag{3.14}$$

The pressure drop across a regular hexagonal duct of length L has been obtained by Asako et al. [8] using a numerical method, as

$$\Delta p = (L/a)(2f\rho_f v_f^2) \tag{3.15}$$

where the small entrance effects have been ignored and $f = 15.065Re^{-1}$ is the friction factor for fully developed flows. Equation (3.15) holds for a honeycomb heat sink of length L where the average fluid velocity v_f is connected to the free stream velocity v_0 by

$$v_f = v_0(1+t/2a)^2. \tag{3.16}$$

3.5. Overall heat transfer coefficient h̄

The total heat transfer rate from the system is $Q = \dot{m}c_p(T_e-T_0)$ which, by noting that $T_e = T_f(L)$, becomes

$$Q = \rho_f v_0 c_p HW(T_w-T_0)\{1-\exp(-L/L^*)\}. \tag{3.17}$$

The overall heat transfer coefficient $\bar{h}$ of the heat sink is defined as [2, 10]

$$\bar{h} = \frac{Q}{2LW\Delta T_m} \tag{3.18}$$

where ΔT_m is the logarithmic mean temperature difference:

$$\Delta T_m = \frac{(T_w-T_0)-(T_w-T_e)}{\ln[(T_w-T_0)/(T_w-T_e)]}. \tag{3.19}$$

It can be readily verified from equations (3.11), (3.13) and (3.19) that $\Delta T_m = T_w-\bar{T}_f$. The resulting expression for $\bar{h}$ is

$$\bar{h} = h\left\{1-\frac{t}{a}+\frac{t}{a}\sqrt{\frac{6}{Bi}}\tanh(\sqrt{2\,Bi/3}H/t)\right\}. \tag{3.20}$$

In the field of electronic packaging, the inverse of $\bar{h}$, $\bar{h}^{-1}$, is commonly known as the thermal resistance of the system [11].

4. Constant heat flux surfaces

We repeat in this section the heat transfer analysis for the model of Fig. 1, assuming that the plates holding the chips release uniform heat flux q_0 in the direction normal to the plate surfaces. Let T_w continue to represent the temperature of the plates, except that it now depends on the spatial coordinate x.

4.1. A single corrugated wall without fins

In the absence of fin attachments, equation (3.1) governing the variation of cell wall temperature for a corrugated wall (Fig. 1(c)) is solved with the boundary conditions

$$-\lambda_s \frac{dT}{d\xi} = \frac{\sqrt{3}}{2} q_0, \quad \text{at } \xi = 0 \tag{4.1a}$$

$$\lambda_s \frac{dT}{d\xi} = \frac{\sqrt{3}}{2} q_0, \quad \text{at } \xi = \frac{2}{\sqrt{3}} H \tag{4.1b}$$

to get

$$T(x,\xi) = T_f(x) + \frac{q_0}{2h\sqrt{2/3\,Bi}} \frac{\cosh\{\sqrt{2\,Bi}(H/\sqrt{3}-\xi)/t\}}{\sinh(\sqrt{2\,Bi/3}H/t)}. \tag{4.2}$$

It follows that the corrugated wall has an average temperature

$$\bar{T}(x) = T_f(x) + \frac{3q_0}{4h}\frac{t}{H} \tag{4.3}$$

and that the temperature difference between the plate surface and fluid, $T_w(x) - T_f(x)$, is

$$T_w(x) - T_f(x) = \frac{q_0 t}{2\lambda_s\sqrt{2\,Bi/3}} \tanh^{-1}(\sqrt{2\,Bi/3}H/t). \tag{4.4}$$

Notice that $T_w(x) - T_f(x)$ is independent of x, an intrinsic feature of heat transfer in ducts with isoflux walls.

4.2. Effects of fins

The effect of fin attachments on the thermal fields inside the heat sink with isoflux plates is analysed first for the simplified model of Fig. 1(d), as in the case of isothermal plates. The solutions to the variation of temperature $T(x,\xi)$ along the corrugated wall and $T(x,\eta)$ along the fin, subjected to the boundary conditions (3.21) and that $T = T_n$ at $\eta = 0$, $dT/d\eta = 0$ at $\eta = l/2$ and $dT/d\eta = 2dT/d\xi$ at $\eta = 0$, are

$$T(x,\xi) = T_f(x) + \frac{\sqrt{3}q_0}{2\lambda_s m}\left\{-\sinh m\xi + \cosh m\xi \frac{[\sinh ml + \frac{1}{2}\cosh ml \tanh(ml/2)]^{-1} + \sinh ml}{\cosh ml}\right\} \tag{4.5a}$$

and

$$T(x,\eta) = T_f(x) + \frac{\sqrt{3}q_0}{2\lambda_s m} \times \frac{\cosh[m(l/2-\eta)]}{\cosh(ml/2)[\sinh ml + \frac{1}{2}\cosh ml \tanh(ml/2)]} \tag{4.5b}$$

where $m = \sqrt{2\,Bi}/t$. The temperature difference between the plate surface and fluid is

$$T_w(x) - T_f(x) = \frac{\sqrt{3}q_0}{2\lambda_s m} \times \frac{[\sinh ml + \frac{1}{2}\cosh ml \tanh(ml/2)]^{-1} + \sinh ml}{\cosh ml}. \tag{4.6}$$

In the absence of fins, equation (4.4) can be rewritten as

$$T_w(x) - T_f(x) = \frac{\sqrt{3}q_0}{2\lambda_s m} \tanh^{-1}(ml). \tag{4.7a}$$

For the corrugated wall model of Fig. 1(d), the temperature difference $T_w - T_f$ as given by equation (4.7a) neglects the contribution from fin attachments, hence represents an overestimation under Type II boundary conditions. As the length of the fin is 1/4 of that of the corrugated wall, it is expected that $T_w - T_f$ is smaller than that given by equation (4.7a) and is approximately given by

$$T_w(x) - T_f(x) = \frac{1}{(1+1/4)} \frac{\sqrt{3}q_0}{2\lambda_s m} \tanh^{-1}(ml). \tag{4.7b}$$

When $0.1 < ml < 1$, the exact solution (4.6) can be replaced by the approximate solution (4.7b) with an error less than 10%. For a corrugated wall with many fin attachments (Fig. 1(c)), the total fin length is half that of the wall, hence the approximate solution for $T_w - T_f$ is

$$T_w(x) - T_f(x) = \frac{q_0 t}{3\lambda_s\sqrt{2\,Bi/3}} \tanh^{-1}(\sqrt{2\,Bi/3}H/t). \tag{4.8}$$

The fluid temperature $T_f(x)$ is a linear function of x and is obtained by an energy balance analysis similar to that leading to equation (3.9), as

$$T_f(x) = T_0 + \frac{2q_0 x}{\rho_f c_p v_0 H}. \tag{4.9}$$

4.3. Overall heat transfer coefficient $\bar{h}$

The overall heat transfer coefficient $\bar{h}$ is again defined according to equation (3.18). It can be readily shown that the logarithmic mean temperature difference ΔT_m for the isoflux plates is simply $T_w - \bar{T}_f$. Thus, from equation (3.18) we can write

$$2LW\bar{h}[T_w(x) - T_f(x)] = L[N_s\sqrt{3}q_0 t + q_w(x)] \tag{4.10}$$

where $q_w(x)$ is given in equation (3.10). The left-hand-side of equation (4.10) is the rate of heat lost to the cooling medium via convection, which must be balanced by the rate of heat input from the source—the right-hand-side of equation (4.10). The resulting expression for $\bar{h}$ is identical to that given by equation (3.20), but its magnitude is different as the local heat transfer coefficient h in each case differs. For developed laminar flows in a

regular hexagonal duct with uniform heat flux along the walls, the local heat transfer coefficient is [7]

$$h = 4.021\frac{\lambda_f}{a}. \tag{4.11}$$

Equations (3.15) and (3.16) continue to apply for the pressure drop across the heat sink.

The maximum temperature of the plate surface occurs at its trailing edge $x = L$, with

$$T_w(L) = T_0 + q_0\left(\frac{2L}{\rho_f c_p v_0 H} + \frac{1}{\bar{h}}\right). \tag{4.12}$$

The thermal design objective of any heat sink associated with isoflux surfaces is to maximise the overall heat transfer coefficient $\bar{h}$ such that $T_w(L)$ is contained within safe operating temperature limits.

5. Heat transfer efficiency

5.1 Comparison with ducts without honeycombs

It is of convenience to non-dimensionalise the overall heat transfer coefficient $\bar{h}$ for a honeycomb heat sink as

$$\frac{\bar{h}}{\lambda_s/a} = \left(\frac{c\lambda_f}{\lambda_s}\right)\left\{1 - \frac{t}{a} + \left(\frac{6\lambda_s}{c\lambda_f}\frac{t}{a}\right)^{1/2}\tanh\left[\frac{H}{a}\left(\frac{3\lambda_s}{2c\lambda_f}\frac{t}{a}\right)^{-1/2}\right]\right\} \tag{5.1}$$

where $c = 3.353$ if isothermal boundary condition holds and $c = 4.021$ if isoflux condition holds. When $\lambda_s \gg \lambda_f$, $H \gg a$ and $a \gg t$ (which are expected to be satisfied by typical micro-cell aluminium honeycombs), equation (5.1) simplifies to

$$\frac{\bar{h}}{\lambda_s/a} = \left(\frac{6c\lambda_f}{\lambda_s}\frac{t}{a}\right)^{1/2}\tanh\left[\frac{H}{a}\left(\frac{3\lambda_s}{2c\lambda_f}\frac{t}{a}\right)^{-1/2}\right]. \tag{5.2}$$

The predicted overall heat transfer coefficient for aluminium honeycombs with $\lambda_s = 200$ W (m^{-1} K^{-1}) and $a = 1$ mm is displayed as a function of t/a in Fig. 2(a) for air cooling and Fig. 2(b) for water cooling. Both isothermal and isoflux boundary conditions are considered and two values of the ratio of heat sink thickness to cell size H/a are selected: 10 and 20. The overall heat transfer coefficient $\bar{h}$ for isoflux condition is about 20% larger than when the plate surfaces are isothermal, and $\bar{h}$ increases as H/a increases. In the absence of honeycombs, the overall heat transfer coefficient of a duct consisting of parallel plates of spacing H is $\bar{h}_1 = c_1\lambda_f/2H$ where $c_1 = 7.54$ of the plates are isothermal and $c_1 = 8.235$ if the plates release constant heat flux [6]. Thus, $\bar{h}_1$ is typically of the order of 10^1 W (m^{-2} K^{-1}) for air cooling and 10^2 W (m^{-2} K^{-1}) for water cooling, which is about two order of magnitudes smaller than when the duct is made of the same plates but with a metal honeycomb core.

5.2. Comparison with open-celled metal foams

If, instead of honeycombs, the heat sink is made of a three-dimensional, open celled metal foam (e.g., ERG Duocel® aluminium foam) sandwiched between two isothermal plates, its overall heat transfer coefficient becomes [2]

$$\frac{\bar{h}_{foam}}{\lambda_s/a} = 1.682\left(Pr^{1/3}\frac{\lambda_f}{\lambda_s}\right)^{1/2}\left(\frac{v_0 a}{\nu_f}\right)^{0.3}\frac{\rho^{1/2}}{(1.535\rho^{-1/2} - 1)^{0.3}} \tag{5.3}$$

where a is the cell size and ρ is the relative density of the foam. For a regular honeycomb, $\rho = 2t/a$ (if $a \gg t$). Selected results of the ratio, $\bar{h}/\bar{h}_{foam}$, suggest that for forced air cooling, metal honeycombs compete well against metal foams with open cells, especially when the relative density is small ($\rho < 0.1$). The behaviour depends weakly on air velocity, with $\bar{h}/\bar{h}_{foam} \propto {v_0}^{-0.3}$. For water cooling, metal foams are about twice as efficient as metal honeycombs.

The flows are essentially laminar in honeycombs and turbulent in metal foams (due to the presence of sharp cell edges [2]). However, at the same relative density level, the surface area density of a honeycomb is in general much larger than that of the metal foam ($\alpha = 2\sqrt{3}\rho^{1/2}/t$ for honeycomb and $\alpha_{foam} = 2\sqrt{3\pi}\rho^{1/2}/a$ for metal foam). This may explain why compact heat exchangers made of micro-cell honeycombs with laminar flows are competing well against those made of metal foams with turbulent flows. Notice also that the pressure drop of laminar flow across a honeycomb ($\Delta p \propto v_0$) is relatively small compared to that of turbulent flow across a metal foam where $\Delta p \propto v_0^{1.6}$ [2–4], potentially an advantage when the flow velocity is large both in terms of constraints on pump/air handler and flow induced noise.

It is worth mentioning that the heat transfer model proposed by Lu, Stone and Ashby (LSA) [2] for metal foams is based on a cubic array of ligaments, thermally correlated with a bank of cylinders. In reality, the cell morphology of a typical metal foam (e.g., ERG Duocel®) is perhaps more adequately represented by an ordered array of tetrakaidecahedra with non-circular, possibly sharp-edged ligaments [3–4]. The LSA model predicts correct trends of heat transfer, but overestimates the total heat transfer rate when compared with experimental measurements. Accordingly, empirical proportionality coefficients are needed to represent the effective solid thermal conductivity and the cell edge diameter [3, 4]. The present model for calculating thermal transport in a metal honeycomb is much more accurate—the cell morphology is represented correctly, the laminar flow based local heat transfer coefficient as well as the pressure drop are obtainable numerically, and the solution based on the corrugated wall model is exact except for the effects of fin attachments.

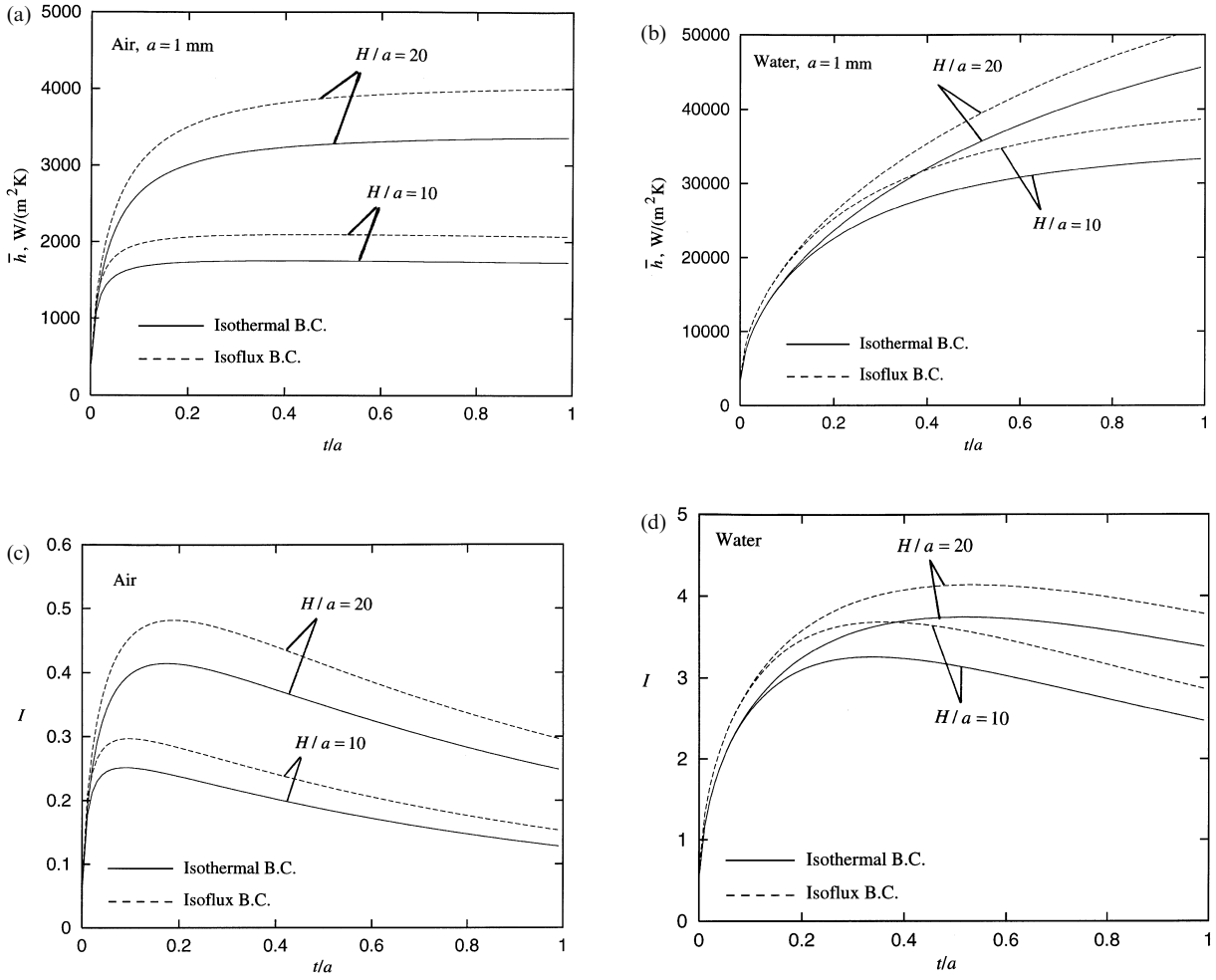

Fig. 2. (a) Overall heat transfer coefficient of a heat sink made of regular aluminium honeycomb plotted as a function of t/a for air cooling and (b) water cooling; the cell size is fixed at $a = 1$ mm. (c) Scaling index I plotted as a function of t/a for air cooling and (d) water cooling.

5.3. Effects of cell orientation and double cell wall thickness

The heat transfer model shown in Fig. 1 assumes that the hexagonal cell is oriented in a way that two cell walls are parallel to the substrates. If the cell is rotated 90° relative to the y-axis so that the two walls are now perpendicular to the substrates (Fig. 1(b)), how would the heat removal efficiency of the honeycomb change? The answer is that the total heat transfer rate decreases, with a new overall heat transfer coefficient given by

$$\bar{h} = h\left\{1 - \frac{t}{a} + \frac{5}{6}\frac{t}{a}\sqrt{\frac{2}{Bi}}\tanh(3\sqrt{Bi/8}H/t)\right\}. \tag{5.4}$$

This result is obtained by following the same analytical procedures as those leading to equation (3.20), and it is valid for both isothermal and isoflux conditions. The characteristic length scale of the problem increases to $L^* = \rho_f c_p v_0 H/2L\bar{h}$, hence the fluid temperature decreases [cf. equation (3.11)]. Thus, the cell orientation as depicted in Fig. 1(b) with two horizontal cell walls is favoured over other orientations for best heat transfer efficiency.

Commercially available micro-cell honeycombs usually consist of regular hexagonal cells having thickness t for four walls and double thickness $2t$ for the other two walls (Fig. 1(b)). In this case, the model of corrugated wall with fin attachments shown in Fig. 1(c) is still valid except for replacing the thickness of the fins with $2t$. Without giving details, it is found that this model leads to an overall heat transfer coefficient identical to that for a regular honeycomb with uniform wall thickness, i.e., equation (4.13).

6. Optimal thermal design

6.1. Order of magnitude analysis

To address the issue of the existence of an optimal cell morphology that would maximise the heat transfer performance of a metal honeycomb, we first perform an order of magnitude analysis similar to that described by Bejan [7, 12] for a stack of parallel boards cooled by laminar forced convection. For simplicity, the analysis is restricted to isothermal conditions and it is assumed that the cell walls attain the same constant temperature T_w as that of the substrates. Furthermore, let the physical dimensions of the heat sink be fixed at L, W, H and the pressure drop across the sink be predetermined at Δp (due to specified pump, compressor or air handler). The relative density of the honeycomb is taken to be small ($t/a \ll 1$) so that the cell wall thickness may be ignored.

Consider first the limit when the cell size approaches zero ($a \to 0$). Each hexagonal channel can be considered as an infinitely long duct, with the fluid temperature at the outlet, T_e, approaching the cell wall temperature, T_w. The laminar flow in each channel is fully developed and, from equation (3.15), the average flow velocity is related to the pressure drop by $v_f = a^2\Delta p/2\mu_f L$. The total heat transfer rate from the heat sink, $Q = \dot{m}c_p(T_e - T_0)$, is, therefore,

$$Q \cong \frac{HWL\Delta p\rho_f c_p(T_w - T_0)}{2\mu_f}\left(\frac{a}{L}\right)^2. \tag{6.1a}$$

In the other limit $a \to \infty$, the pressure drop in the honeycomb heat sink is dominated by entrance effects. The mean flow velocity and the average heat transfer coefficient in each channel are $v_f \approx 1.23(\Delta p/\rho_f)^{1/2}$ and $h \approx 1.4(\lambda_f/a)(Re\,Pr\,a/L)^{1/2}$, respectively [8]. The total heat transfer rate can be calculated by multiplying the total number of channels to the heat transfer rate from a single channel, yielding

$$Q \cong 6.21\frac{HW\lambda_f Pr^{1/2}(T_w - T_0)}{L}\left(\frac{\Delta pL^2}{\mu_f v_f}\right)^{1/4}\left(\frac{a}{L}\right)^{-1}. \tag{6.1b}$$

Equations (6.1a) and (6.1b) reveal that the rate of heat lost to the convective medium decreases as a^2 when $a \to 0$ and as a^{-1} when $a \to \infty$. The $Q(a)$ curve in between is unknown, but the optimal cell size a_{opt} at which Q is maximised is surmised to be of the same order as the a value obtained by intersecting the asymptotes (6.1a) and (6.1b). Thus,

$$(a/L)_{opt} \approx 2.32Pr^{1/6}Be^{-1/4} \tag{6.2}$$

where the dimensionless parameter $Be = \Delta pL^2/\mu_f v_f$ is the Bejan number [12, 13]. For the optimal spacing of parallel boards cooled by convection, the same order of magnitude analysis suggests that the coefficient 2.32 in equation (6.2) should be replaced by 2.73 [12]. The result is found to be fairly accurate compared with more exact solutions from numerical calculations [12].

6.2. Effects of finite cell wall thickness

The above order of magnitude analysis neglects the effects of cell wall thickness t and assumes that all cell walls attain uniform temperature T_w. These restrictions will be relaxed below to obtain the optimal relative density (or, equivalently, the optimal t/a) for best heat transfer performance.

A popular measure of the heat transfer performance of a heat sink is the ratio of total heat transfer rate to the pumping power needed to force the fluid through, $\bar{h}/\Delta p$ [2, 14]. The optimal cell morphology of a honeycomb is one that would maximise $\bar{h}/\Delta p$. From equations (3.15) and (4.13), a non-dimensional scaling index I is conveniently introduced as follows

$$\begin{aligned} I &= \frac{\bar{h}}{(\lambda_s/v_f\rho_f v_0)(a/L)\Delta p} \\ &= 0.0332\left(\frac{c\lambda_f}{\lambda_s}\right)\left(1+\frac{t}{2a}\right)^{-2}\left\{1-\frac{t}{a}\right. \\ &\quad \left.+\left(\frac{6\lambda_s}{c\lambda_f}\frac{t}{a}\right)^{1/2}\tanh\left[\frac{H}{a}\left(\frac{3\lambda_s}{2c\lambda_f}\frac{t}{a}\right)^{-1/2}\right]\right\}. \end{aligned} \tag{6.3}$$

The attributes of both finite cell wall thickness and non-uniform thermal fields are accounted for in equation (6.3). The scaling index I is plotted as a function of t/a for air cooling on Fig. 2(c) and for water cooling on Fig. 2(d). Both isothermal and isoflux conditions are used, and the effect of increasing H/a from 10–20 is studied. For air cooling, I is maximised at $t/a \approx 0.05$ if $H/a = 10$, and at $t/a \approx 0.15$ if $H/a = 20$. For water cooling, the maximum of I occurs at much larger values of t/a. Also, changing the isothermal condition to constant-flux condition increases the value of t/a at which I is maximised. In general, the optimal cell morphology, represented here by t/a, is not constant but dependent upon the geometry and heat transfer condition of the heat sink, and the type of convective cooling medium.

For heat exchanger applications where weight is cause for concern, the more appropriate merit index is I/ρ or, equivalently, $I/(t/a)$ as $\rho = 2t/a$ for a regular honeycomb. Hence, I/ρ is maximised when $t/a \to 0$.

7. Concluding remarks

The transport of heat in micro-cell aluminium honeycombs subjected to convective cooling has been analysed using the corrugated wall model. Except for the effects of fin attachments which are modelled approximately, the approach is felt to be fairly accurate. Simple closed form

solutions are obtained for the thermal fields and overall heat transfer coefficient as functions of cell morphological parameters and heat transfer conditions. These are analysed to find the optimal cell morphology for maximum overall heat transfer efficiency. The heat transfer characteristics of a honeycomb are similar to those of metal foams, although the underlying mechanisms are different. In contrast to turbulent flows in metal foams, the streaming of fluid in a honeycomb is essentially laminar—this is nevertheless remunerated by its superior surface area to volume ratio, leading to about two order of magnitudes augmentation in heat dissipation efficiency when an open channel is designed with a metal honeycomb core. The performance would be further improved if a honeycomb heat sink is designed with turbulent flow, although the flow induced noise may become significant. The results are of relevance for thermal management applications in high power electronics where compact and highly efficient heat dissipation media are required.

Acknowledgements

This work was supported by EPSRC and by the ARPA/ONR MURI program on Ultralight Metal Structures (No. N00014-1-96-1028). The author wishes to thank Prof. Mike Ashby for helpful discussions.

References

[1] Hexcel Data Sheets, Hexcel Co., Pleasanton, CA, 1998.
[2] T.J. Lu, H.A. Stone, M.F. Ashby, Heat transfer in open-cell metal foams, Acta mater. 46 (1998) 3619–3635.
[3] A.F. Bastawros, A.G. Evans, Characterisation of open-cell aluminium alloy foams as heat sinks for high power electronic devices, in: Proceedings of the Symposium on the Application of Heat Transfer in Microelectronics Packaging, IMECE, Dallas, Texas, 1997.
[4] A.F. Bastawros, A.G. Evans, H.A. Stone, Evaluation of cellular metal heat dissipation media, Harvard University, Division of Engineering and Applied Sciences Report MECH-325, Cambridge, MA 02138, U.S.A., 1998, to be published.
[5] J.S. Goodling, Microchannel heat exchangers, in: A.M. Khounsary (Ed.), High Power Flux Engineering II, SPIE Conf. Proc., 1997.
[6] T.J. Lu, A.G. Evans, J.W. Hutchinson, The effects of material properties on heat dissipation in high power electronics, Trans. ASME, J. Electronic Packaging, 1998 in press.
[7] A. Bejan, Convective Heat Transfer, 2nd ed., Wiley, New York, 1995.
[8] Y. Asako, H. Nakamura, M. Faghri, Developing laminar flow and heat transfer in the entrance region of regular polygonal ducts, Int. J. Heat Mass Transfer 31 (1988) 2590–2593.
[9] R.K. Shah, A.L. London, Laminar Flow: Forced Convection in Ducts, Academic Press, New York, 1978.
[10] J.P. Holman, Heat Transfer, McGraw-Hill Book Company, New York, 1989.
[11] R.W. Knight, J.S. Goodling, D.J. Hall, Optimal thermal design of forced convection heat sinks—analytical, ASME J. Electronic Packaging 113 (1991) 313–321.
[12] A. Bejan, E. Sciubba, The optimal spacing of parallel plates cooled by forced convection, Int. J. Heat Mass Transfer 35 (1992) 329–364.
[13] S. Petrescu, Comments on the optimal spacing of parallel plates cooled by forced convection, Int. J. Heat Mass Transfer 37 (1994) 1283.
[14] M.J. Andrews, L.S. Fletcher, Comparison of several heat transfer enhancement technologies for gas heat exchangers, J. Heat Transfer 118 (1996) 897–902.